UAV Deployable buoy-style sensor for in situ water quality monitoring

Md Asifuzzaman Khan[a], Matthew Burnett[a], Austin R.J. Downey[a,b], Joud N. Satme[a], and Jasim Imran[b]

[a]Department of Mechanical Engineering, University of South Carolina, Columbia, USA
[b]Department of Civil and Environmental Engineering, University of South Carolina, Columbia, USA

ABSTRACT

The current standard for detecting contamination in water bodies relies on manual sampling and off-site laboratory analysis, resulting in delays in disseminating critical public health information. This paper presents a novel approach to real-time, in situ water quality monitoring using a UAV-deployable, long-endurance sensor cluster. At the core of the system is an open-source sensor integrated into a buoy, referred to as a sensor node, designed to measure key water quality parameters including pH, total dissolved solids, turbidity, and temperature. The sensor node is built from low-cost, modular hardware, enabling rapid deployment and system adaptability. It features long-range bidirectional wireless communication, GPS for localization, and an energy-efficient power management system. A solar charging module extends the node's operational endurance. To overcome the logistical challenges of large-scale sensor deployment, an autonomous UAV-based drop mechanism is integrated for efficient distribution across water bodies. A field demonstration was conducted in an urban creek affected by overland runoff. Sensor readings showed deviations of 0.71–4.2% compared to industrial reference instruments, indicating high accuracy. The system operated continuously for 17.5 hours on battery power alone, and energy analysis showed that the solar module could generate approximately 1.8 times the node's average power consumption, suggesting potential for indefinite operation under typical sunlight conditions.

Keywords: real-time monitoring, UAV-deployable, water quality, sensor nodes, wireless communication, open-source

1. INTRODUCTION

Rapid urbanization has contributed significantly to water pollution. Some key sources of contamination include industrial effluents, agricultural runoff, and domestic wastewater. Industrial effluents often contain hazardous chemicals and heavy metals, which pose severe threats to aquatic ecosystems and human health.[1] Agricultural activities contribute to water pollution through the runoff of pesticides, fertilizers, and animal waste, leading to nutrient overloads and eutrophication.[2] Additionally, Domestic wastewater also contributes a wide range of organic and inorganic pollutants.[3] Discharges from these sources affect water quality by altering pH, Total dissolved Solids (TDS), and turbidity beyond accepted levels for safe use. Effective water quality management[4] is imperative to mitigate these adverse effects. It ensures the protection of aquatic habitats, preservation of biodiversity,[5] and safeguarding public health by providing clean and safe drinking water. Additionally, maintaining high water quality is vital for recreational activities such as watersports and for promoting the sustainable development .[6] To address these challenges, in situ water quality monitoring is crucial.

Further author information: (Send correspondence to Austin Downey)
Austin Downey: Email: austindowney@sc.edu

The conventional approach to water quality monitoring involves selecting sampling locations, collecting water samples, and transporting them to a laboratory for analysis. Spatial interpolation techniques, such as kriging,[7] are then used to estimate values across the water body. However, this method is labor-intensive, time-consuming, and does not support real-time analysis.

To enable real-time monitoring, an in situ sensor capable of onboard data processing and wireless transmission is essential. Recent advances in open-source embedded hardware and sensors have made such systems feasible. For example, Koparan et al.[8] developed a UAV-based system that lands on water surfaces to collect data, which is stored on an SD card with time and location metadata. While this reduces manual deployment effort, it still lacks real-time capability, as the UAV must return to retrieve data. Additionally, contact with contaminated water poses health risks to the operator. Kinar and Brinkmann[9] proposed an in situ sensor with onboard processing, GPS, and cellular IoT communication. While effective in urban areas, this approach is limited in remote or disaster-affected regions without reliable cellular coverage.

This paper presents the design[10] of a UAV-deployable in situ water quality sensor package that transmits real-time data via a dedicated wireless network. The sensor node integrates probes for pH, electrical conductivity, temperature, and turbidity, and is deployed using a UAV. Once deployed, it wirelessly transmits data to a base station, allowing the UAV to return without contacting the water. This setup enables rapid deployment in hazardous or inaccessible locations. The sensor node includes GPS for time and location tagging, and a solar-powered buoy that provides both energy harvesting and buoyancy for stable operation.

The contributions of this study are twofold: (1) the development of a compact, UAV-deployable in situ water quality sensor using open-source hardware and software, and (2) performance validation through experimental deployment in creek affected by urban runoff.

2. METHODOLOGY

This section reports the sensor node's physical design, embedded hardware, and deployment mechanism.

2.1 Sensor node design

The sensor node is designed as a vertically oriented floating device consisting of three visible sections: a submerged sensing section at the bottom, an exposed communication and power input section at the top, and a solar buoy in the middle. Figure 1 presents a horizontal view of the fully assembled sensor node.

The right side of Figure 1 represents the top portion of the sensor node, which remains above the water surface. This section houses the primary electronic components such as the main controller board, GPS, and radio communication module as depicted in Figure 2(a). The electronics are placed in a 3D printed chassis and the chassis is enclosed with a schedule 40 clear PVC pipe that slides into the chassis from the top. There is a groove for the O-ring at the top of the chassis that seals the contact between the chassis and PVC pipe providing water resistance. A solar power input port, utilizing a waterproof JST connector; and a wireless antenna port, utilizing an SMA female connector, are exposed out of the chassis' top face. Their contacts with the chassis are water-proofed using epoxy.

The left side of Figure 1 represents the bottom portion of the sensor node, which remains submerged in water during operation. This section houses multiple water quality sensors enclosed by a 3D-printed grated protective cap. The protective cap allows water to flow while shielding the sensors from debris and external impacts. The sensors integrated into this portion include a temperature probe, pH probe, electrical conductivity probe, and turbidity sensor, as illustrated in Figure 2(b). These sensors are mounted through holes situated at the bottom of the chassis. Then the bottom end of the the PVC union is placed around it and epoxy is poured. The epoxy helps to waterproof the contact surfaces between the chassis, sensors, and PVC union. The other end of the PVC union is connected to the clear PVC pipe that slides in from the top. There is an O-ring between the two ends of the PVC union that ensures a watertight modular attachment for easy maintenance and battery replacement.

The solar buoy's position is vertically adjustable to maintain the sensor node's upright balance in water. Nine solar panels are installed in grooves, wired in three series-connected groups, and then linked in parallel. The buoy's hollow space is filled with expanding foam for buoyancy and waterproofing. Its position can be adjusted to achieve optimal vertical balance.

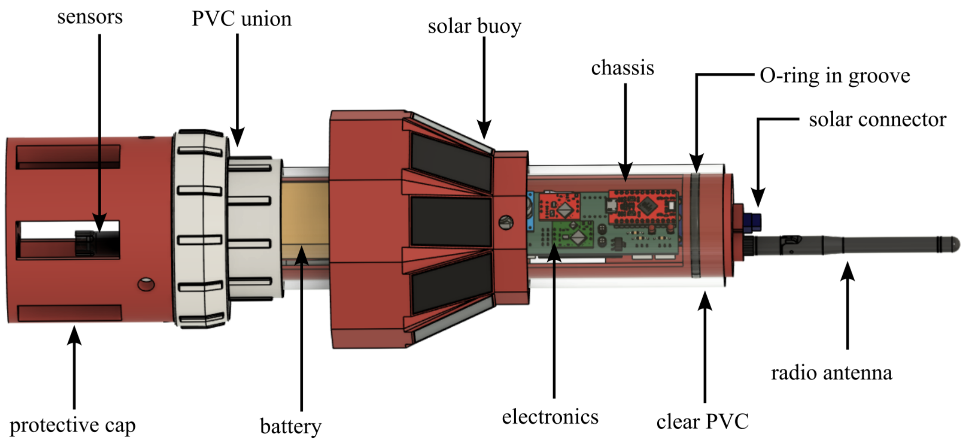

Figure 1. Horizontal view of the fully assembled sensor node. The left side represents the bottom portion, and the right side represents the top portion, with a solar buoy illustrated in the middle.

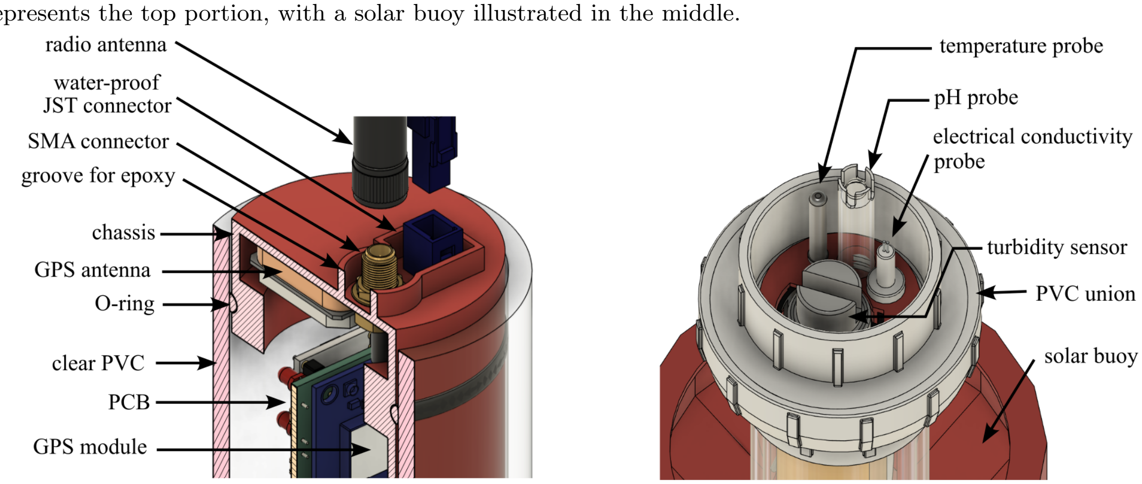

(a) (b)

Figure 2. Ends of the sensor package, showing:(a) the cross-section of the top portion displaying internal electronics and external connectors, and (b) the bottom view of the sensor node without the protective cap, displaying the measurement sensors.

2.2 Embedded system overview

The embedded system diagram of the sensor node is illustrated in Figure 3. The sensor node is managed by an 8-bit 16 MHz Atmega32U4 processor onboard the Sparkfun ProMicro microcontroller. The peripheral devices communicate with the microcontroller using various serial communication protocols. To condition the analog signal taken from the pH and conductivity probes, their respective conditioning module manufactured by Atlas Scientific is used. They use the Inter-Integrated Circuit (I^2C) protocol to communicate with the microcontroller. The electrical conductivity module is programmed to output electrical conductivity reading in µS/cm. However, it can be programmed to provide readings on Total Dissolved Solids (TDS) in ppm. To get the temperature data, a waterproof DS18B20 temperature sensor is used which communicates with the microcontroller using 1-wire protocol and provides temperature data directly in °C unit. To get turbidity reading an Amphenol TSD-10 turbidity sensor is used. A turbidity sensor measures the cloudiness or haziness of a liquid by detecting the amount of light scattered by suspended particles. It consists of an infrared LED and a photodetector positioned at an angle to measure scattered light. When the turbidity increases, more light is scattered, and the photodetector outputs a higher voltage value, which indicates the concentration of suspended particles in the fluid. The relationship between turbidity (N) in Nephelometric Turbidity Units (NTU) and voltage output (V) from the turbidity sensor can be described using

$$V = -0.008N + V_0, \tag{1}$$

where V_0 is the voltage that the turbidity sensor reads while placed in clear water (0 NTU). V_0 is measured to be around 3.7 V for the turbidity sensor used in this work.

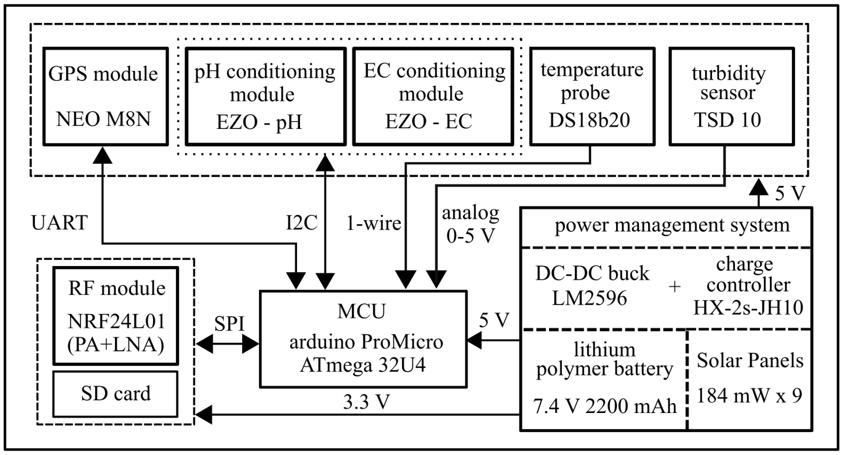

Figure 3. Embedded system diagram of the sensor node.

The microcontroller gets position data from a u-blox NEO-M8N GPS module connected by the Universal Asynchronous Receiver/Transmitter (UART) protocol. This module also has a built-in Real-Time-Clock (RTC) onboard that provides time stamps against recorded sensor data. The microcontroller then transmits the position, time stamp, and sensor readings wirelessly utilizing a long-range nRF24L01+PA+LNA (Power Amplifier + Low Noise Amplifier) radio communication module designed by Nordic Semiconductor. The transmitted data is received by a base station similar to the design used by Chowdhury et al.[11] for soil moisture monitoring in levees. If the sensor is out of the base station's range, the microcontroller saves the time stamp, position, and sensor data onboard a micro SD card. Both the nRF24L01+PA+LNA wireless module and the micro SD card utilize the Serial Peripheral Interface (SPI) protocol to communicate with the microcontroller.

The entire sensor node is powered by a 7.4 V 2200 mAh lithium polymer battery. A buck converter converts the battery voltage to 5 V as most electronics onboard are powered by a 5 V voltage level. The micro SD card and nRF24 module require 3.3V to operate and it is acquired by feeding 5 V to a linear 3.3 V regulator. To increase operational endurance, the sensor node is equipped with nine 184 mW SM141K06TF solar panels. Solar power goes into the battery via a Battery Management System (BMS) that helps to balance-charge the lithium polymer battery during daytime. The microcontroller reads water quality data (pH, turbidity, conductivity, temperature) once every 30 s. For the rest of the idle time, it cuts off power to the peripheral devices to extend battery life using a solid-state switch.

2.3 Drone deployment mechanism

The sensor node is deployed into the water using an Electro-Permanent Magnet (EPM) mounted on the UAV. An Electro-Permanent Magnet (EPM) is a type of electromagnet that can switch between magnetized and demagnetized states using a brief electrical pulse. Unlike typical electromagnets, an EPM can retain its magnetization without constant energy input. Smith et al. proposed a UAV-deployable stage height sensor[12] leveraging EPM. A similar but inverted mechanism is implemented here, as shown in Figure 4. The UAV carries an EPM on its underside between the landing gear legs, while the buoy features a metal plate on its outer wall. This mechanism ensures secure docking of the sensor node when the EPM is magnetized. The UAV navigates using GPS and can be programmed to demagnetize the EPM at a desired location automatically. Once the EPM is demagnetized, the sensor node falls freely into the water due to gravity. Due to its bottom-heavy design, it sinks upright, with the buoy keeping the top side above water, ensuring the antenna remains exposed.

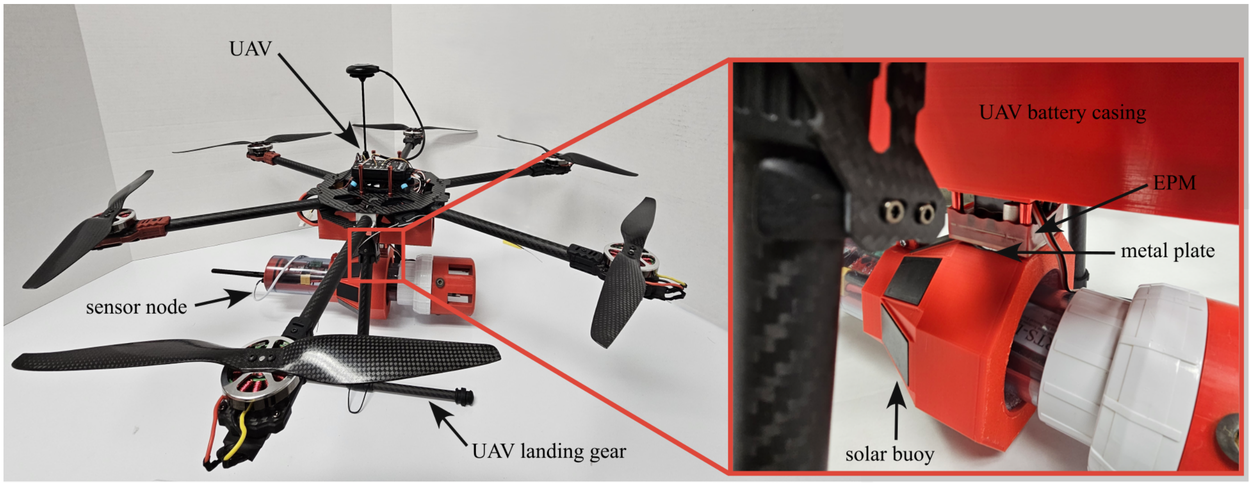

Figure 4. Sensor node docked under a hexacopter UAV with EPM-based deployment mechanism shown on the right.

3. RESULTS

Before proceeding with the in situ test, a benchtop test was performed to verify the accuracy of the pH, conductivity, and temperature sensors. To compare the pH and conductivity, respective industrial sensors from VIVOSUN were used. The error in pH was found around 0.71% and in TDS, around 4.22%. Temperature sensor validation was conducted by comparing the DS18B20 sensor to a Type K thermocouple. This test revealed an error percentage of 1.15%. The data from these tests are outlined in Table 1

Table 1. Sensor node's data comparison with reference sensors.

parameters	sensor node's value	reference sensor's value	error (%)
pH	7.01	6.96	0.71
electrical conductivity (µS/cm)	12619	12108	4.22
temperature (°C)	25.7	26	1.15

After the benchtop test, the sensor node was deployed in a creek in downtown Columbia, South Carolina, where urban runoffs flow through as shown in Figure 5. It was deployed with the solar power connector disconnected to test the endurance just on battery power. It lasted about 17.5 h at a sampling rate of two samples per minute. The time series plot of sensor data from the creek is shown in Figure 6.

The sensor was deployed at midday during the early Spring of 2025 and ran continuously for the next 17.5 h. The outlier data points related to sensor startup right after the deployment were omitted, as the sensor node suddenly comes in contact with water and causes large spikes in sensor values. The fall in temperature is observed as nightfall begins after approximately 5 h. The conductivity reading stays between 95 to 115 µS/cm, which is well within the range of 38 to 1074 µS/cm for urban runoffs.[13] The pH was found within the acceptable range of 5.5 to 8. However, it was observed that as night falls, both pH and conductivity data exhibit a downward trend, possibly indicating a change in the effluents in the water as work hours conclude.

The sensor ran for a total of 17.5 h on a 2200 mAh battery, which resulted in an average current consumption of 125.71 mA at 7.4 V. So the average energy consumption results in 930.254 mW. Considering the nominal power of the solar panels, which is specified by the manufacturer to be 184 mW each, the total solar power from all nine modules amounts to 1656 mW. This is almost 1.8 times the average power consumption when using only battery power. So, in theory, the solar buoy should be able to power the sensor node indefinitely in normal sunshine conditions.

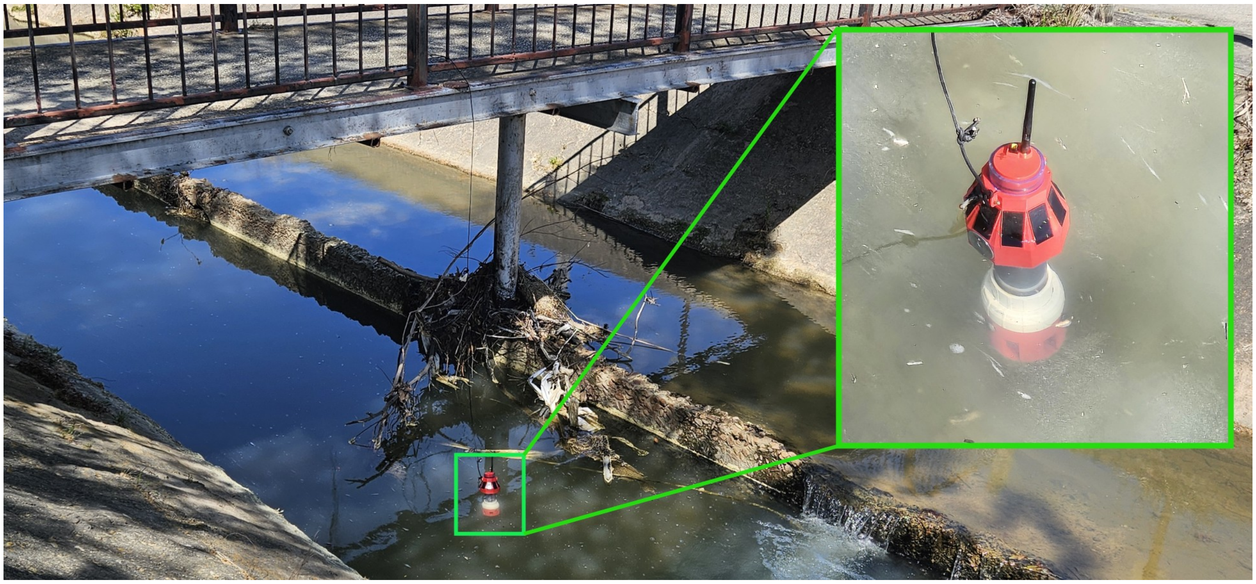

Figure 5. A sensor node deployed in a creek, tied with a string to take a stable photo.

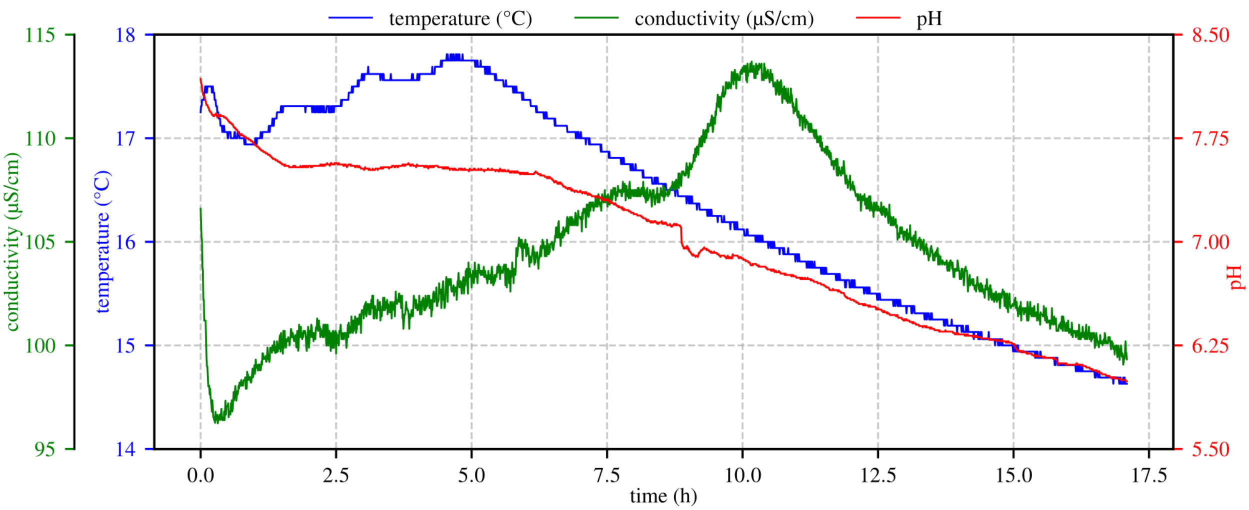

Figure 6. Time series plot of sensor data from a creek showing continuous 17.5 h of run-time without solar power.

4. CONCLUSION

The proposed UAV-deployable in situ water quality sensor package streamlines water quality assessment by eliminating manual sample collection and retrieval. It enables real-time monitoring and wireless data transmission, reducing human involvement and associated health risks while improving deployment efficiency.

Benchtop validation showed that the sensor node produced accurate readings, closely aligning with industrial reference sensors for pH, electrical conductivity, and temperature. In situ deployment in an urban runoff creek further confirmed system reliability, with continuous operation for 17.5 hours on battery power alone. Observed variations in pH and conductivity demonstrated the system's ability to detect real-time changes in water quality. Energy analysis suggests that the solar buoy could theoretically sustain indefinite operation under ideal sunlight conditions.

Future work will focus on optimizing power management to improve energy efficiency under variable conditions. As pH, conductivity, and turbidity are temperature-dependent, future designs will incorporate temperature compensation to improve accuracy. Additionally, a networked cluster of sensor nodes using advanced wireless protocols will be developed to enable synchronized, large-scale monitoring across multiple sites. These enhancements aim to improve the system's scalability, reliability, and long-term utility in diverse and challenging environments.

ACKNOWLEDGMENTS

This work is supported by the National Science Foundation, United States Grant numbers CMMI - 2152896 and ITE - 2344357 The support of the National Science Foundation is gratefully acknowledged. Any opinions, findings, conclusions, or recommendations expressed in this material are those of the authors and do not necessarily reflect the views of the National Science Foundation.

REFERENCES

[1] Bervoets, L., Baillieul, M., Blust, R., De Boeck, G., and Verheyen, R., "Impact assessment of industrial effluents on freshwater ecosystems," *Science of The Total Environment* **134**, 1123–1128 (Jan. 1993).

[2] Wiens, J., "Agricultural runoff and water pollution," *Canadian Water Resources Journal* **5**, 78–89 (Jan. 1980).

[3] Tsuzuki, Y., "An index directly indicates land-based pollutant load contributions of domestic wastewater to the water pollution and its application," *Science of The Total Environment* **370**, 425–440 (Nov. 2006).

[4] Behmel, S., Damour, M., Ludwig, R., and Rodriguez, M., "Water quality monitoring strategies — a review and future perspectives," *Science of The Total Environment* **571**, 1312–1329 (Nov. 2016).

[5] Irfan, S. and Alatawi, A. M. M., "Aquatic ecosystem and biodiversity: A review," *Open Journal of Ecology* **09**(01), 1–13 (2019).

[6] Dodds, W. K., Bouska, W. W., Eitzmann, J. L., Pilger, T. J., Pitts, K. L., Riley, A. J., Schloesser, J. T., and Thornbrugh, D. J., "Eutrophication of U.S. freshwaters: Analysis of potential economic damages," *Environmental Science and Technology* **43**, 12–19 (Nov. 2008).

[7] Khan, M., Almazah, M. M. A., EIlahi, A., Niaz, R., Al-Rezami, A. Y., and Zaman, B., "Spatial interpolation of water quality index based on ordinary kriging and universal kriging," *Geomatics, Natural Hazards and Risk* **14** (Mar. 2023).

[8] Koparan, C., Koc, A., Privette, C., and Sawyer, C., "In situ water quality measurements using an unmanned aerial vehicle (UAV) system," *Water* **10**, 264 (Mar. 2018).

[9] Kinar, N. J. and Brinkmann, M., "Development of a sensor and measurement platform for water quality observations: design, sensor integration, 3d printing, and open-source hardware," *Environmental Monitoring and Assessment* **194** (Feb. 2022).

[10] ARTS-Lab, "In-situ-water-quality-sensor." GitHub.

[11] Chowdhury, P., Crews, J., Mokhtar, A., Oruganti, S. D. R., Wyk, R. V., Downey, A. R. J., Flemming, M., Bakos, J. D., Imran, J., and Khan, S., "Distributed real-time soil saturation assessment in levees using a network of wireless sensor packages with conductivity probes," in [*Volume 11: Safety Engineering, Risk and Reliability Analysis; Research Posters*], *IMECE2024*, American Society of Mechanical Engineers (Nov. 2024).

[12] Smith, C., Satme, J., Martin, J., Downey, A. R., Vitzilaios, N., and Imran, J., "UAV rapidly-deployable stage sensor with electro-permanent magnet docking mechanism for flood monitoring in undersampled watersheds," *HardwareX* **12**, e00325 (Oct. 2022).

[13] Masoner, J. R., Kolpin, D. W., Cozzarelli, I. M., Barber, L. B., Burden, D. S., Foreman, W. T., Forshay, K. J., Furlong, E. T., Groves, J. F., Hladik, M. L., Hopton, M. E., Jaeschke, J. B., Keefe, S. H., Krabbenhoft, D. P., Lowrance, R., Romanok, K. M., Rus, D. L., Selbig, W. R., Williams, B. H., and Bradley, P. M., "Urban stormwater: An overlooked pathway of extensive mixed contaminants to surface and groundwaters in the united states," *Environmental Science and Technology* **53**, 10070–10081 (Aug. 2019).